minerals

MDPI

Article

Characterization Analysis of Airborne Particulates from Australian Underground Coal Mines Using the Mineral Liberation Analyser

Nikky LaBranche [1,*], Kellie Teale [2], Elaine Wightman [2], Kelly Johnstone [3] and David Cliff [1]

[1] Minerals Industry Safety and Health Centre, Sustainable Minerals Institute, The University of Queensland, 47A Sir James Foots Building, Brisbane, QLD 4072, Australia; d.cliff@uq.edu.au
[2] Julius Kruttschnitt Mineral Research Centre, Sustainable Minerals Institute, The University of Queensland, 40 Isles Rd, Indooroopilly, Brisbane, QLD 4068, Australia; k.white@uq.edu.au (K.T.); e.wightman@uq.edu.au (E.W.)
[3] School of Earth and Environmental Sciences, The University of Queensland, Chamberlin Building (35), Brisbane, QLD 4072, Australia; k.johnstone2@uq.edu.au
* Correspondence: n.labranche@uq.edu.au; Tel.: +61-4-0761-0108

Abstract: Exposure monitoring and health surveillance of coal mine workers has been improved in Australia since coal workers' pneumoconiosis was reidentified in 2015 in Queensland. Regional variations in the prevalence of mine dust lung disease have been observed, prompting a more detailed look into the size, shape, and mineralogical classes of the dust that workers are being exposed to. This study collected respirable samples of ambient air from three operating coal mines in Queensland and New South Wales for characterization analysis using the Mineral Liberation Analyser (MLA), a type of scanning electron microscope (SEM) that uses a combination of the backscattered electron (BSE) image and characteristic X-rays for mineral identification. This research identified 25 different minerals present in the coal samples with varying particle size distributions for the overall samples and the individual mineralogies. While Mine 8 was very consistent in mineralogy with a high carbon content, Mine 6 and 7 were found to differ more significantly by location within the mine.

Keywords: coal mine dust lung disease; coal workers pneumoconiosis; particle characterization; mineral liberation analyser

Citation: LaBranche, N.; Teale, K.; Wightman, E.; Johnstone, K.; Cliff, D. Characterization Analysis of Airborne Particulates from Australian Underground Coal Mines Using the Mineral Liberation Analyser. *Minerals* **2022**, *12*, 796. https://doi.org/10.3390/min12070796

Academic Editor: Fernando Rocha

Received: 27 May 2022
Accepted: 21 June 2022
Published: 22 June 2022

1. Introduction

Coal workers' pneumoconiosis and other mine dust lung diseases have seen a resurgence both in Australia and the United States. In Australia, coal workers pneumoconiosis (CWP) was re-identified more recently in 2015, and since then 267 mine dust lung disease cases have been reported [1,2]. The US has had two decades of increases in both the prevalence and severity of disease [3]. There have been high levels of regional variability, with miners in central Appalachia being disproportionately affected [3–8]. This has prompted new research to characterize dust exposures in both the US and Australian underground coal mines [9–12].

The history of exposure monitoring for and the setting of exposure standards for respirable coal dust and silica in coal mines has been detailed in a previous paper [13]. Characterization work was previously undertaken in the 1980's but was limited by the technology available at the time [14,15]. Particle size distributions could only be calculated for the overall sample. The mineralogy was only analyzed for a select few minerals already known to be present. Today's technology allows for information to be gathered on individual particles. This allows for particle size distributions to be calculated for each mineralogy and every mineral present to be identified.

Coal contains several minerals as a result of depositional conditions within peat-mire and/or precipitation of porewaters or penetrated fluids during post-coalification [16].

Therefore, coal dust contains a complex mixture of mineralogical classes from various sources within the mines [17]. Previous studies have used scanning electron microscopy with energy dispersive X-ray (SEM-EDX) to characterize mineralogy and size distributions of respirable coal mine dust, especially in the USA [9,10,16,17] and Australia [12], and well as other countries [18–21]. This work has demonstrated that there can be other sources of respirable dust within a mine in addition to the coal seam and an understanding of the mineralogical components, including the silica is needed. The dust characterization present in underground coal mines should be quantified as the dust characteristics can vary widely between and even within mines, which has implications for the health hazards of that dust. It has already been demonstrated that the size of the dust may affect the health hazard [22].

Following on from this work, characterization analysis was conducted on the FEI Quanta 600 Mk2 Minerals Liberation Analyser (MLA) (Hillsboro, OR, USA), another type of scanning electron microscope (SEM) energy dispersive spectra (EDS) X-ray mineral identification. MLA analysis is typically performed on samples encased in a block of epoxy resin. This work analyses the particles collected on a filter from the ambient air using respirable cyclone elutriators. This paper aims to show the validity of the MLA for analyzing airborne particulate samples taken of the respirable fraction of dust from underground coal mines in Australia.

2. Materials and Methods

Respirable dust samples were collected from ambient air in three Australian underground coal mines in the two major coal mining states of Queensland and New South Wales. All mines sampled are producing metallurgical grade coal. These mines all operate longwall faces and used miner bolter machines. In Australia, separate mining and bolting units are generally only used for bord and pillar mining, also known as room and pillar in the US. No further information can be given about the mine locations due to their request for anonymity. The collection of the ambient air samples underground using respirable cyclone elutriators generally followed the procedure and protocols used in recent sampling efforts in US coal mines and the first round of Australian samples analyzed in the US by SEM-EDX [9,10,12,16,17].

A total of 28 samples were collected from 12 locations over three mine sites and seven testing days, as shown in Table 1. These are labeled Mines 6–8 as the Mines 1–5 samples were analyzed in the previous paper using the Virginia Tech Methodology [12]. The Mine 8 samples were taken in quadruplicate, while singular samples were taken for Mines 6 and 7. This was done because of timelines and personnel allowed to visit the mines due to the pandemic. Some samples could not be analyzed due to overloading and for several samples only mineralogy could be obtained as the loading resulted in a skewed particle size distribution (PSD). Mineralogy is available for 17 of the 28 samples, while reliable PSD data is available for 11 samples.

Samples were taken in a variety of locations in the underground mines which are listed in Table 1. These included on the longwall, around the continuous miners, on the shuttle car, and during secondary recovery activities. On the longwall, the sampling locations included the area where operators are normally present just by the maingate corner of the longwall as well as around the midface of the longwall. The shuttle car carries coal from the continuous miner to a grizzly which feeds onto the belt line that takes it out of the mine, which is normally within a few hundred meters of the continuous miner.

Samples were collected with Casella Higgins-Dewell type plastic respirable cyclone elutriators (SKU 116000B) on Zefon 37 mm polycarbonate filters with 0.4 micron pore size, both ordered through AirMet Scientific (Newstead, QLD, Australia). Cassettes and cyclones were packed in the laboratory of the Sustainable Minerals Institute at The University of Queensland (UQ). These were either flown to the mine site for sampling in checked baggage or mailed to the person collecting the samples. After collection, filters were removed from the Casella cassettes inside the cyclone elutriators and placed in 37 mm polystyrene cassettes for return transport in carry-on luggage or mailed back in the Casella

cassettes. Once received in the mail the filters were removed from the Cassella cassettes that the sample was collected in and were then placed into the 37 mm polystyrene cassettes for storage.

Table 1. Sampling Set Information.

Test No.	Mine No.	Test Day	Samples Analyzed	Location Code	Location
1	6	1	1	MG	Longwall maingate
2	6	1	1	MF	Longwall midface
3	6	2	1	CM	Continuous Miner
4	6	2	1	SR	Secondary recovery activity
5	6	3	1	CM	Continuous Miner
6	7	4	1	MF	Longwall midface
7	7	5	1	MF	Longwall midface
8	8	6	2	CM	Continuous Miner
9	8	6	2	CM	Continuous Miner
10	8	6	2	SC	Shuttle car cab
11	8	7	2	MF	Longwall midface
12	8	7	2	MG	Longwall maingate

The sampling in Queensland mines used SKC AirChek 3000 pumps (Eighty Four, Pa, USA) while Casella Apex 2 pumps (Kemptson, Bedford, United Kingdom) were used in the New South Wales Mines. Pumps used in Queensland were field calibrated with an SKC Field rotameter (within calibration). All pumps were operated at the required flow rate of 2.2 L/min in line with the requirements of Australian Standard 2985 [23]. Photos of the sampling frame setup and an example of the frame mounted on a continuous miner during sampling can be found in the previous paper [12]. The sampling frames were mounted as close as practicable to what would be the worker breathing height during the sampling (approximately 1.5 m height).

All filters were delivered to the laboratory at the Julius Kruttschnitt Mineral Research Centre (JKMRC) for analysis using the Mineral Liberation Analyser. These filters were mounted to aluminum stubs, and a carbon coating was applied, as shown in Figure 1. Six regions were analyzed across the filter. An average of 550,000 particles were analyzed per filter with a total of over 8.5 million particles identified on the 17 samples. An FEI Quanta 650 MLA equipped with a Bruker Silicon Drift Detector was used to measure the samples using the XBSE measurement mode [24]. The system was operated with a 13 mm working distance and an accelerating voltage of 25 kV at a resolution of 0.28 μm per pixel.

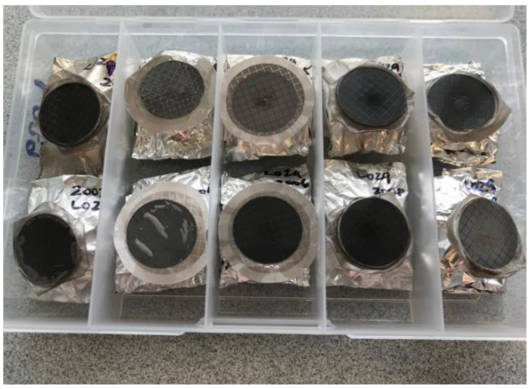

Figure 1. Filter papers mounted to aluminum stubs.

There were 25 different minerals included in the mineral reference library plus an unknown and low counts category. Between 142,000 and 758,000 particles were analyzed per filter. Each of these particles were classified by matching the characteristic X-ray collected during MLA measurement to the mineral reference library. The elemental composition of the minerals included in the mineral reference library is shown in Table 2, these generally use the stoichiometric composition and standard mineral formulae. The mineral list contains both minerals and mineral groups as well as elemental carbon and the manmade compound, stainless steel. The MLA can identify composite particles (i.e., those particles that contain more than one mineral) and images of all the classified particles are available in the MLA software, Dataview 3.1.4.686. The particle size distributions by minerals that were calculated for this paper are filtered for particles that contain more than 50% of the mineral in question. It is possible that a few particles are excluded from the particle size distributions (PSDs) by mineral because there was no single mineral that accounted for over 50% of the particle. All particles are included in the overall particle size distributions.

Table 2. MLA mineral reference library, elemental composition.

Mineral	IMA Abbrev	Density	Formula	Al (%)	Ca (%)	Cl (%)	Cr (%)	Cu (%)	F (%)	Fe (%)	H (%)	K (%)	Mg (%)	Na (%)	Ni (%)	O (%)	P (%)	S (%)	Si (%)	Ti (%)	Unknown (%)	Zr (%)
Chalcopyrite	Ccp	4.2	$CuFe_2S_2$	0	0	0	0	34.62	0	30.43	0	0	0	0	0	0	0	34.94	0	0	0	0
Pyrite	Py	5.01	FeS_2	0	0	0	0	0	0	46.54	0	0	0	0	0	0	0	53.46	0	0	0	0
Chlorite *	Chl	3	CLO_2^-	8.72	0	0	0	0	0	18.05	1.3	0	11.78	0	0	46.53	0	0	13.62	0	0	0
Muscovite	Ms	2.83	$KAl_2(Si_3Al)O_{10}(OH)_2$	20.3	0	0	0	0	0.95	0	0.45	9.8	0	0	0	47.36	0	0	21.13	0	0	0
Amphibole *	Amp	3.4	$Mg_7Si_8O_{22}(OH)_2$	3	18.02	0	0	0	0	0	0	0	7.88	0	0	45.06	0	0	26.03	0	0	0
Quartz	Qz	2.63	SiO_2	0	0	0	0	0	0	0	0	0	0	0	0	53.26	0	0	46.74	0	0	0
Plagioclase *	Pl	2.62	$Na(AlSiO_3O_8)$	10.29	0	0	0	0	0	0	0	0	0	8.77	0	48.81	0	0	32.13	0	0	0
Orthoclase	Or	2.56	$K(AlSi_3O_8.)$	9.69	0	0	0	0	0	0	0	14.04	0	0	0	45.99	0	0	30.28	0	0	0
Kaolinite	Kln	2.6	$Al_2Si_2O_5(OH)_4$	20.9	0	0	0	0	0	0	1.56	0	0	0	0	55.79	0	0	21.75	0	0	0
Zircon	Zrn	4.65	$Zr(SiO_4)$	0	0	0	0	0	0	0	0	0	0	0	0	34.91	0	0	15.32	0	0	49.76
Magnesium Silicate	---	3.3	$MgSiO_3$	0	0	0	0	0	0	0	0	0	24.22	0	0	47.81	0	0	27.98	0	0	0
Calcium Silicate	---	3.9	$Ca_3Fe^{3+}{}_2(SiO_4)_3$	0	23.65	0	0	0	0	21.97	0	0	0	0	0	37.79	0	0	16.58	0	0	0
Clinochlore	Clc	2.65	$Mg_6Al(AlSi_3O_{10})(OH)_8$	13.18	0	0	0	0	0	9.09	1.31	0	15.83	0	0	46.88	0	0	13.72	0	0	0
Iron Oxide	---	5.2	Fe_2O_3	0	0	0	0	0	0	72	0	0	0	0	0	28	0	0	0	0	0	0
Magnesium Oxide	---	3.8	MgO	0	0	0	0	0	0	0	3.6	0	41.6	0	0	54.8	0	0	0	0	0	0
Aluminium Oxide	---	3.04	AlO(OH)	44.97	0	0	0	0	0	0	1.68	0	0	0	0	53.35	0	0	0	0	0	0
Ilmenite	Ilm	4.72	$Fe^{2+}Ti^{4+}O_3$	0	0	0	0	0	0	36.8	0	0	0	0	0	31.64	0	0	0	31.56	0	0
Stainless Steel **	---	7.8	FeCr...	0	0	0	16	0	0	67	0	0	0	0	10	0	0	0	0	0	0	0
Aluminium	Al	2.7	Al	100	0	0	0	0	0	0	0	0	0	0	0	0	0	0	0	0	0	0
Calcite	Cal	2.71	$Ca(CO_3)$	0	35	0	0	0	0	0	0	0	0	0	0	65	0	0	0	0	0	0
Gypsum	Gp	2.3	$Ca(SO_4)\cdot 2H_2O$	0	23.27	0	0	0	0	0	2.34	0	0	0	0	55.77	0	0	18.62	0	0	0
Sylvite	Syl	1.99	KCl	0	0	47.55	0	0	0	0	0	52.45	0	0	0	0	0	0	0	0	0	0
Halite	Hl	2.17	NaCl	0	0	60.67	0	0	0	0	0	0	0	39.33	0	0	0	0	0	0	0	0
Apatite *	Ap	3.19	$Ca_5(PO_4)(F,Cl,OH)$	0	39.37	2.32	0	0	1.24	0	0.06	0	0	0	0	38.76	18.25	0	0	0	0	0
Carbon ***	---	2.26	C	0	0	0	0	0	0	0	0	0	0	0	0	0	0	0	0	0	0	0
Unknown		3		0	0	0	0	0	0	0	0	0	0	0	0	0	0	0	0	0	100	0
Low_Counts		0		0	0	0	0	0	0	0	0	0	0	0	0	0	0	0	0	0	100	0
No_XRay		0		0	0	0	0	0	0	0	0	0	0	0	0	0	0	0	0	0	100	0

* Mineral Group; ** Manmade Compound; *** Element.

Each filter for characterization analysis was given a unique filter ID and location data is added to make up its sample code. The sample code starts with the mine number, which

is 6, 7, or 8 in this case, the two letters for the location code and the last two digits of the filter ID. The location coding includes longwall maingate (MG), longwall mid-face (MF), continuous miner (CM), shuttle car (SC), and secondary recovery (SR) as shown in Table 1. For example, the code for the first sample is 6SR_01, which is from Mine 6, from secondary recovery activities, and is filter number 2001.

3. Results

Similar to the characterization performed previously on samples from Mines 1–4 [12], the relative mineral abundance for Mines 6–8 was found to differ between mines as well as at various locations within a mine Figure 2 shows the mineralogy classes for the samples from Mines 6–8 that were analyzed in this phase of the study.

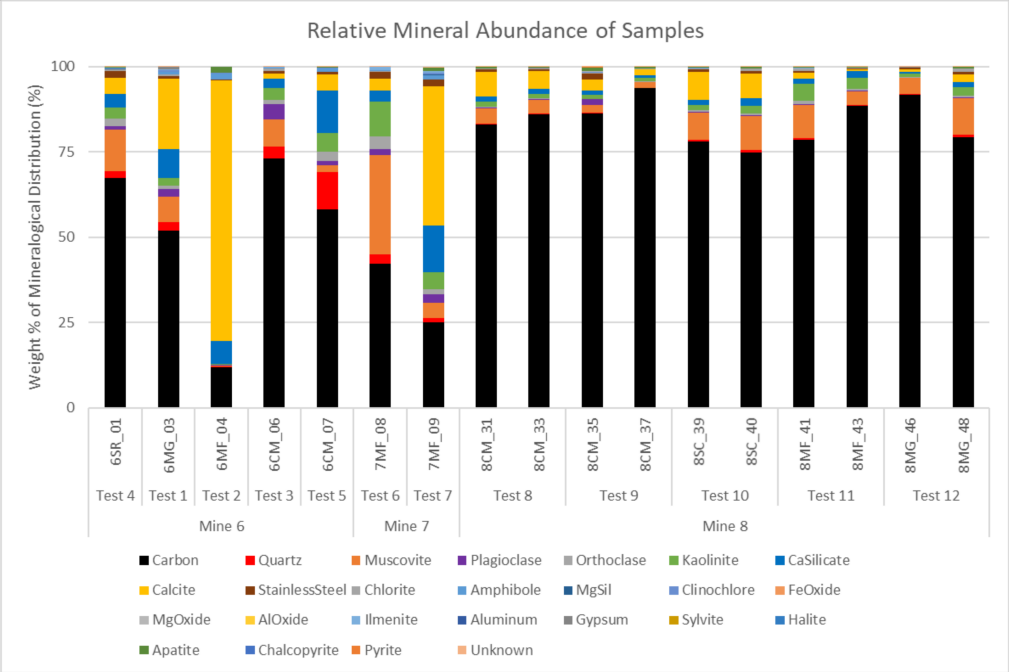

Figure 2. Relative Mineral Abundance of Samples for Mines 6–8.

The samples from Mine 8 contain a significant amount of carbon, ranging from 75–92%. Mines 6 and 7 have a much lower and more variable percentage of carbon material. The carbon identified in these samples consists mainly of coal and diesel particulate matter (DPM). It is not possible to differentiate between coal and DPM with the MLA as it is only identifying the presence of carbon, however, these particles can be differentiated optically, due to the DPM being agglomerated chains of nanosized particles. There are large proportions of calcite in the midface samples in Mine 6 and one of the Mine 7 midface samples. The two longwall midface samples from Mine 7 were taken on different days and reflect the changes in the mineralogy over the time period. The two continuous miner samples in Mine 6 were also taken on different days and show variability in mineralogy. There is good agreement between the paired samples taken in Mine 8. The quartz content is shown in red. Mine 8 has very little quartz content while Mines 6 and 7 show a slightly higher percentage of quartz.

Figure 3 shows the overall particle size distribution of the Mine 6 samples with the equivalent circle diameter in microns plotted against the cumulative passing weight percentage calculated by the MLA. There is a much wider spread in the overall particle size distribution for Mine 6. The coarsest PSD is that of the continuous miner (CM) sample, represented by the dashed line. There was slight overloading on this filter where a small number of overlapping particles were being interpreted by the MLA as larger particles, so sample 6CM_06 has been filtered to remove the particles greater than 13 microns. The

maingate samples have a coarser PSD than the midface sample. Both of these trends are consistent with the general findings of relative PSD in Mines 1–4 in the previous paper [12]. However, the PSDs are not directly comparable between papers in the current format as Mines 1–4 are based on the cumulative percentage of particles by count and this paper uses cumulative passing weight percentage. The particle size distributions for Mine 7 are not shown due to the amount of overloading on some of the filters.

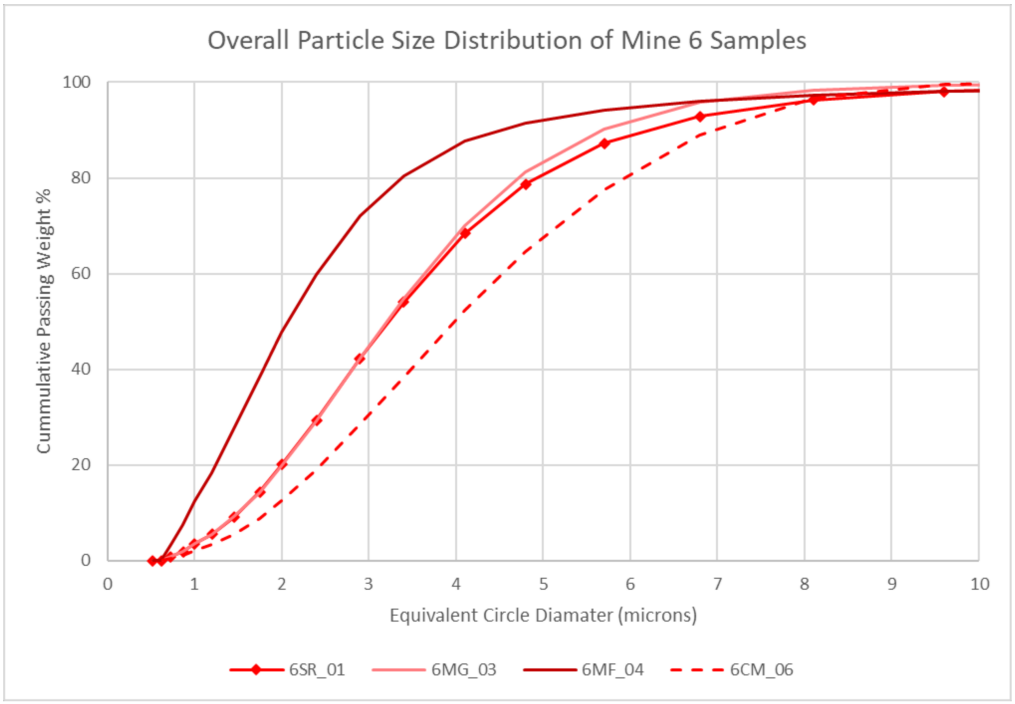

Figure 3. Cumulative Particle Size Distribution for Mine 6 Samples.

Figure 4 shows the overall particle size distribution of the samples from Mine 8. These samples show a much tighter PSD with less variability between locations in the mine.

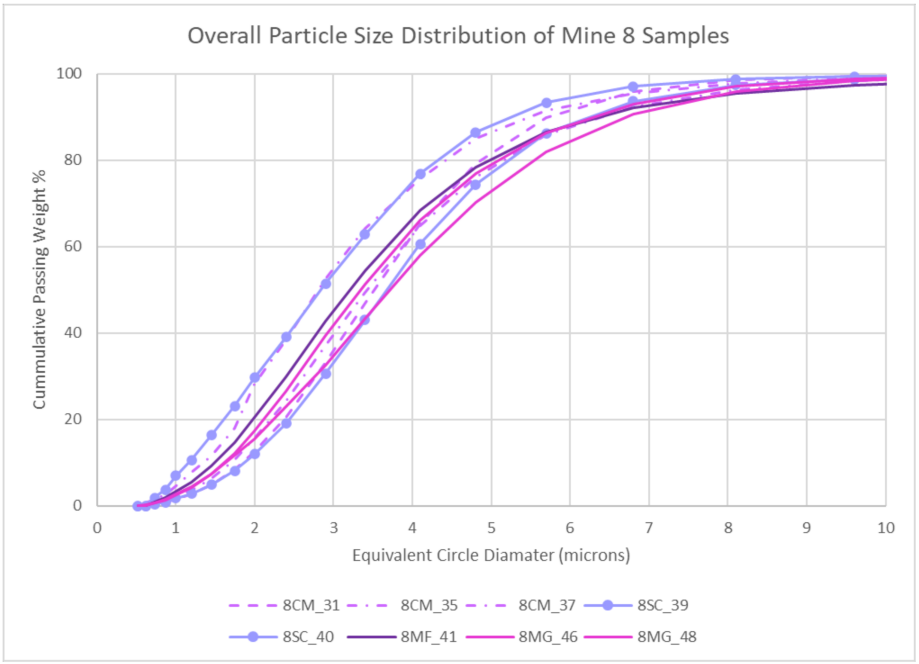

Figure 4. Cumulative Particle Size Distribution for Mine 8 Samples.

Figure 5 shows the overall particle size distribution of all the samples. The difference in the spread between PSDs is much more noticeable when combined, with Mine 6 having both coarser and finer PSDs than Mine 8. The PSDs for Mine 7 were not able to be calculated due to the overloading of the samples. Mine 8 does not seem to follow the same trends in the PSD progressively getting finer from continuous miner to maingate to midface samples, but this could also be an artifact of how low the variability is in the PSDs for this mine.

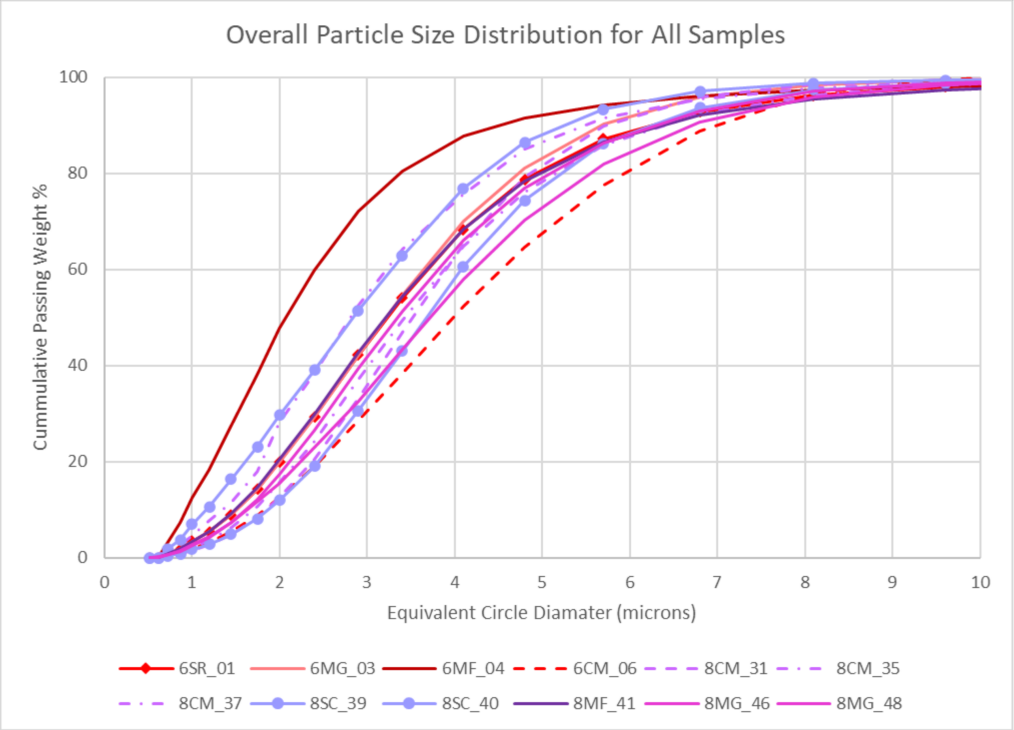

Figure 5. Overall Particle Size Distribution for All Samples.

The MLA is able to analyze the individual dust particles and determine the PSD of each mineral class. The MLA software defaults to calculating the PSD of any particles that contain any amount of a given mineral. For the purposes of this paper the data has been filtered to include only particles that have >50% by weight of a certain mineral, thus only calculating the PSD for particles that are predominately that mineral. It is possible that some particles will not be included in any PSD apart from the overall PSD if there is no dominant mineral above 50% weight, for example, if a particle contains three minerals of roughly equal weight percent.

Figure 6 shows the PSD distribution for the particles with >50% weight of quartz. The quartz fraction is usually finer than the overall particle size distribution. The Mine 6 midface sample has an especially fine PSD with 90% of the particles less than 3 microns equivalent circle diameter. Similar to the overall PSD, Mine 8 also has a tighter PSD of quartz than does Mine 6.

The PSD of several of the mineralogical components is shown in Figure 7 for various samples. There were 25 different mineralogies identified which are listed above in Figure 2. For the purposes of showing the variability in PSDs, the predominant minerals have been selected here including carbon, quartz, muscovite, plagioclase, orthoclase, kaolinite, calcium silicate, and calcite.

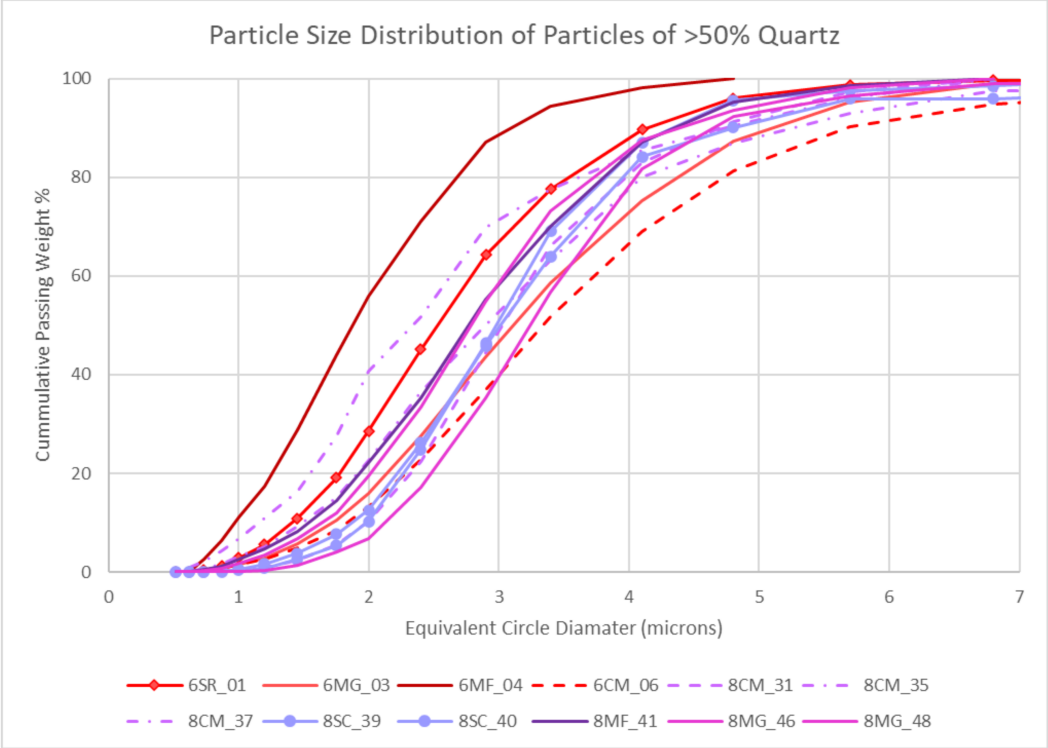

Figure 6. Particle size distribution of Particles with >50% weight of Quartz (Silica).

Stainless steel has also been included in the PSDs by mineral as it was not expected to be found in the samples. The fraction of stainless steel varied from 0.02 to 1.2% percentage in these samples. The actual number of particles containing any stainless steel ranges from 158 to 6180 per filter. None of the mining machines (i.e., continuous miner, longwall) contain stainless steel that could be identified as the source and it has been theorized that these particles may be coming from the diesel engines of the personal transport vehicles that are being operated in the mines. Further investigation is needed into the potential sources of this material.

While the overall PSD of the Mine 6 samples Figure 7a,b varied more significantly between samples, there is not as large a variability in the individual PSDs. The carbon fraction in the Mine 6 secondary recovery sample is coarser than the other mineralogies, but otherwise, the PSDs are very similar. The PSDs for the various mineralogies of the Mine 8 samples have a wider spread. The kaolinite and muscovite, represented by the green and orange lines respectively, have the coarsest PSDs in Figure 7c,d,f. Figure 7e had the narrowest PSD of the Mine 8 samples. As can be seen in all the samples the red lines representing the quartz tend to be on the finer side of the PSDs. The orthoclase, represented by the grey line, also has one of the finest PSDs in Figure 7b–f. The continuous miner and shuttle car samples Figure 7c,d were collected at the same time and show good agreement with very similar PSDs for each mineralogy. Not all mineralogical classes were present in each sample.

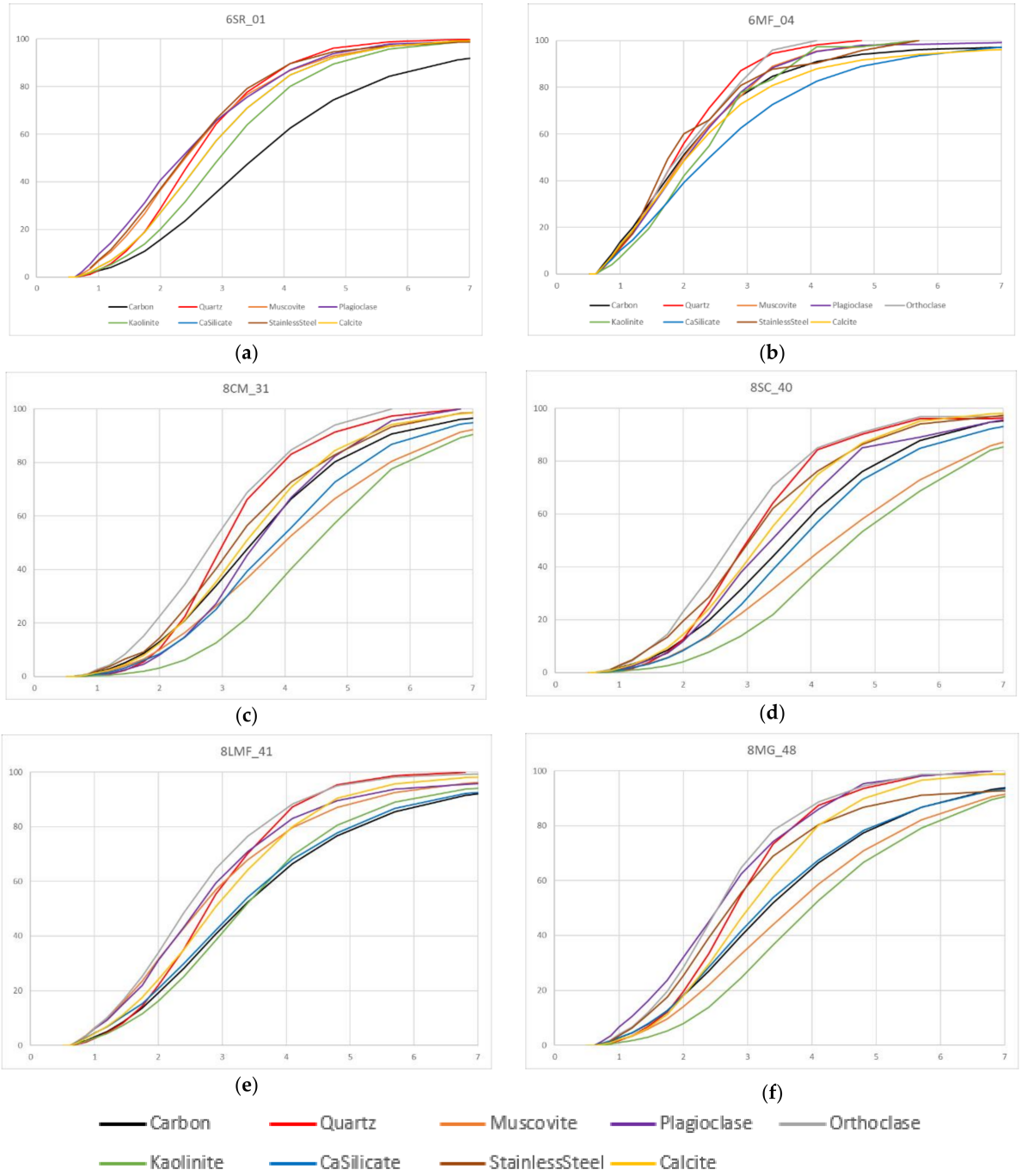

Figure 7. Particle Size Distributions of Various Mineralogical Classes by >50% weight percentage. X-axis = Equivalent Circle Diameter (microns) and Y-axis = Cumulative Passing Weight Percentage. (**a**) Mine 6 Secondary Recovery, (**b**) Mine 6 Longwall Mid-Face, (**c**) Mine 8 Continuous Miner, (**d**) Mine 8 Shuttle Car, (**e**) Mine 8 Longwall Mid-Face, (**f**) Mine 8 Longwall Maingate.

4. Discussion

The standard MLA sample preparation technique is to create a sample block by encasing ore in epoxy resin. The ore is often crushed prior to being encased in the block. The sample blocks can then be cut on various planes to provide a surface for analysis. The sample preparation for airborne particulate matter is significantly different in that dust from the ambient air is collected on a filter with a respirable cyclone elutriator. The MLA has been used for airborne particulate matter on filter in one previous instance, which was with environmental samples of the inhalable size fraction taken at an iron-ore mine

in Brazil [25]. These samples are the first respirable samples on the filter from Australian underground coal mines to be analyzed on the MLA. Figure 8 shows a backscattered electron (BSE) image from one of the filters.

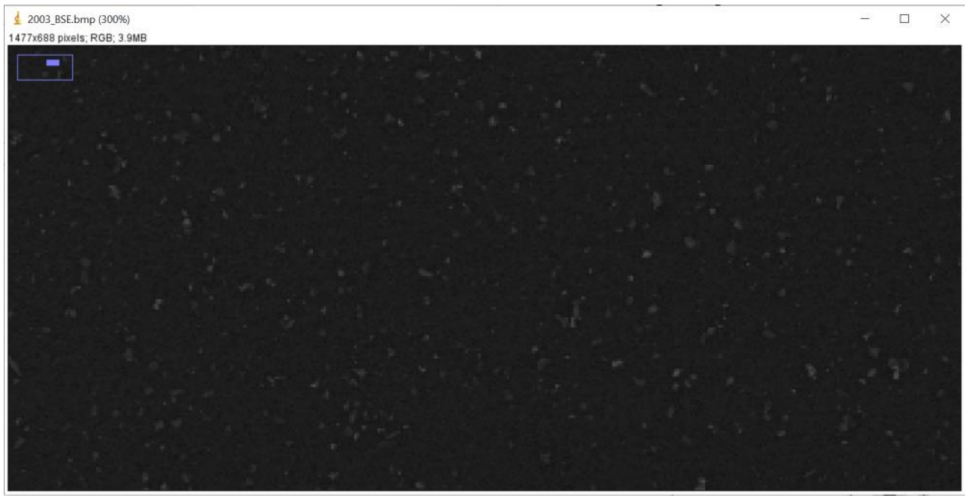

Figure 8. BSE Image of Ambient Air Particles on Filter.

The MLA provides measurements of the individual particles and includes mapping of the minerals within the particles, as shown in Figure 9. Airborne particulate matter sampling such as this requires that the polycarbonate filters not be overloaded, or the MLA cannot distinguish between the particles and will start aggregating them and treating them as larger particles. These issues can be picked up by looking at the images of the particles and noticing the presence of 'holes' in the particles, which is actually a gap between different particles. The MLA methodology also suffers from the same limitation in the inability to differentiate the carbon fraction between coal and diesel particulate matter (DPM), which was discussed in more detail in the previous work [12].

Similar to the findings for Mines 1–4 [12], the mineralogies present were found to vary more significantly by mine and to a lesser extent by location within individual mines. The noted variation in mine dust lung disease prevalence rates by region and the variations in geology found make characterization a promising technique for better understanding the relationship between dust exposure and disease. Several types of aluminosilicate particles including muscovite, kaolinite, plagioclase, and orthoclase were identified in the samples. A significant quantity of aluminosilicates have been found during the analysis of lung particle burden and there is currently no exposure standard for this class of particulates [26]. The shape of the particles was generally found to be ovaloid with a few elongate particles (high length to width ratio).

The mineral class, size, and shape of the particle present in the environment may correlate to varying levels of health hazards of the dust being generated with the ambient air of the mine. Mine dust lung disease prevalence rates have been found to vary by mine and region and the logical next step in establishing that correlation lies in the characterization of the dust [13]. This characterization work serves as an important precursor to future research needs to determine the extent of the variation in toxicity. Simply crushing and analyzing a coal sample may not be enough given the variety of sizes and mineralogies present from different sources. The cumulative effect of these may be different from that of the individual components [27,28]. The collection of samples can easily be done using the same cyclone elutriators that are used regularly in the mines for compliance monitoring. A specialized filter for microscopy analysis and a shorter duration of sampling is needed. Work is being done to standardize the MLA analysis methodology to decrease the amount of time for sample preparation and scanning and ensure repeatability of results.

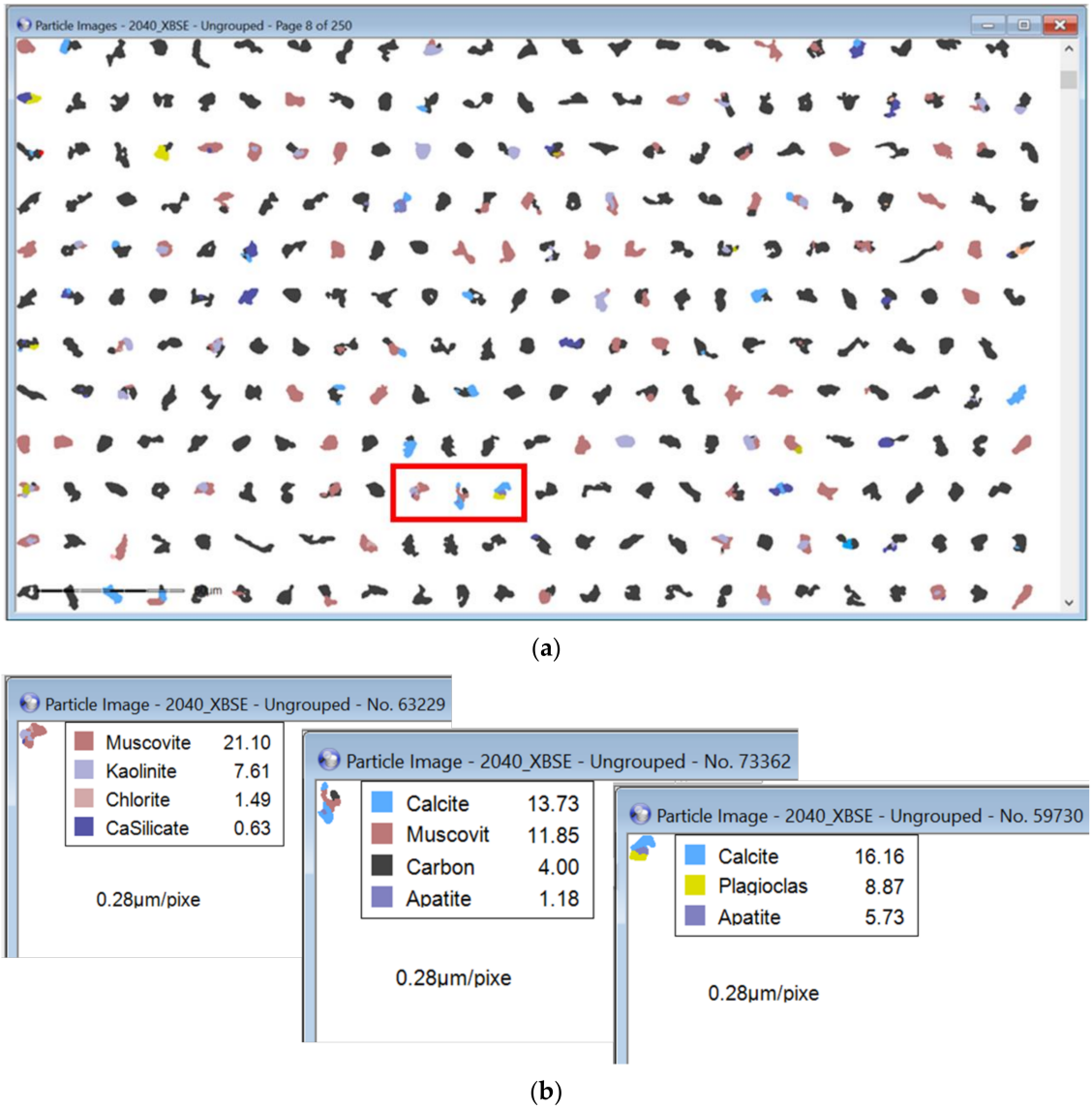

Figure 9. MLA Images of Individual Particles for Sample 8SC_40. (**a**) MLA False Color Images of Particles for Sample 8SC_40. (**b**) Map of Select Individual Particles for Sample 8SC_40.

The variation in PSD indicates that simple mass/gravimetric measurements of dust may not be sufficient to protect all workers. Some tasks may expose workers to a higher number of finer particles that penetrate deeper into the lungs while other workers may be exposed to a smaller number of coarser particles despite there being a similar mass of respirable dust. Furthering the understanding of the variation in particle burden may improve exposure monitoring and control to reduce this risk in the future.

5. Conclusions

Various sources of dust within the mine will differ in their mineralogy and particle size distributions and may cause variability in the health hazard of the dust. Establishing the true exposures of workers through characterization studies such as this will aid further understanding of the health implications and benefit future work in lung deposition and toxicity studies.

The MLA identified 25 mineral classes contained within the dust in three Australian underground coal mines. This study has shown the applicability of the MLA as a tool for understanding the characterization of dust in airborne particulate matter on a filter in the respirable fraction. This method has shown its potential in mining and should be expanded

to more commodities and industries to gain insights into their exposures. Further work has already been undertaken with metalliferous mines and comparisons of the respirable and inhalable size fractions and an expansion of the program is planned.

Author Contributions: Conceptualization, N.L.; methodology, N.L. and K.T.; software, K.T., E.W. and N.L.; validation, K.T., E.W. and N.L.; formal analysis, N.L.; investigation, N.L. and K.T.; resources, N.L. and E.W.; data curation, E.W. and N.L.; writing—original draft preparation, N.L.; writing—review and editing, E.W., K.J. and D.C.; visualization, N.L.; supervision, D.C. and K.J.; project administration, D.C.; funding acquisition, D.C. All authors have read and agreed to the published version of the manuscript.

Funding: This research was funded by The University of Queensland and Resources Safety and Health Queensland.

Acknowledgments: The authors would like to thank the mines for their facilitation of the sample collection visits.

Conflicts of Interest: The authors declare no conflict of interest.

References

1. Coal Workers Pneumoconiosis Select Committee. *Black Lung White Lies: Inquiry into the Re-Identification of Coal Workers' Pneumoconiosis in Queensland*; Queensland Governement: Brisbane, Australia, 2017.
2. Resources Safety & Health Queensland. Mine Dust Lung Diseases. Available online: https://www.business.qld.gov.au/industries/mining-energy-water/resources/safety-health/mining/accidents-incidents/mine-dust-lung-diseases (accessed on 18 May 2022).
3. Blackley, D.J.; Halldin, C.N.; Laney, A.S. Continued Increase in Prevalence of Coal Workers' Pneumoconiosis in the United States, 1970–2017. *Am. J. Public Health* **2018**, *108*, 1220–1222. [CrossRef]
4. Almberg, K.S.; Halldin, C.N.; Blackley, D.J.; Laney, A.S.; Storey, E.; Rose, C.S.; Go, L.H.T.; Cohen, R.A. Progressive Massive Fibrosis Resurgence Identified in U.S. Coal Miners Filing for Black Lung Benefits, 1970–2016. *Ann. Am. Thorac. Soc.* **2018**, *15*, 1420–1426. [CrossRef]
5. Blackley, D.J.; Crum, J.B.; Halldin, C.N.; Storey, E.; Laney, A.S. Resurgence of Progressive Massive Fibrosis in Coal Miners-Eastern Kentucky. *Morb. Mortal. Wkly. Rep.* **2016**, *65*, 1385–1389. [CrossRef] [PubMed]
6. Hall, N.B.; Blackley, D.J.; Halldin, C.N.; Laney, A.S. Current Review of Pneumoconiosis Among US Coal Miners. *Curr. Environ. Health Rep.* **2019**, *6*, 137–147. [CrossRef] [PubMed]
7. Doney, B.C.; Blackley, D.; Hale, J.M.; Halldin, C.; Kurth, L.; Syamlal, G.; Laney, A.S. Respirable coal mine dust in underground mines, United States, 1982–2017. *Am. J. Ind. Med.* **2019**, *62*, 478–485. [CrossRef] [PubMed]
8. Antao, V.C.; Petsonk, E.L.; Sokolow, L.Z.; Wolfe, A.L.; Pinheiro, G.A.; Hale, J.M.; Attfield, M.D. Rapidly progressive coal workers' pneumoconiosis in the United States: Geographic clustering and other factors. *Occup. Environ. Med.* **2005**, *62*, 670–674. [CrossRef] [PubMed]
9. Sarver, E.; Keles, C.; Rezaee, M. Characteristics of respirable dust in eight appalachian coal mines: A dataset including particle size and mineralogy distributions, and metal and trace element mass concentrations. *Data Brief* **2019**, *25*, 104032. [CrossRef] [PubMed]
10. Sarver, E.; Keles, C.; Rezaee, M. Beyond conventional metrics: Comprehensive characterization of respirable coal mine dust. *Int. J. Coal Geol.* **2019**, *207*, 84–95. [CrossRef]
11. The National Academies of Sciences, Engineering, and Medicine. *Monitoring and Sampling Approaches to Assess Underground Coal Mine Dust Exposures*; The National Academies of Sciences, Engineering, and Medicine: Washington, DC, USA, 2018. [CrossRef]
12. LaBranche, N.; Keles, C.; Sarver, E.; Johnstone, K.; Cliff, D. Characterization of Particulates from Australian Underground Coal Mines. *Minerals* **2021**, *11*, 447. [CrossRef]
13. LaBranche, N.; Cliff, D.; Johnstone, K.; Bofinger, C. Respirable Coal Dust and Silica Exposure Standards in Coal Mining: Science or Black Magic? In Proceedings of the Resource Operators Conference 2021, University of Southern Queensland, Queensland, QLD, Australia, 10–12 February 2021; pp. 251–260.
14. Lee, C. *Statistical Analysis of the Size and Elemental Composition of Airborne Coal Mine Dust*; The Pennsylvania State University: State College, PA, USA, 1986.
15. Mutmansky, J.M.; Lee, C. An Analysis of the Size and Elemental Composition of Airborne Coal Mine Dust. In Proceedings of the Coal Mine Dust Conference, West Virginia University, Morgantown, WV, USA, 8–10 October 1984; pp. 235–249.
16. Dai, S.; Hower, J.C.; Finkelman, R.B.; Graham, I.T.; French, D.; Ward, C.R.; Eskenazy, G.; Wei, Q.; Zhao, L. Organic associations of non-mineral elements in coal: A review. *Int. J. Coal Geol.* **2020**, *218*, 103347. [CrossRef]
17. Ward, C.R. Analysis, origin and significance of mineral matter in coal: An updated review. *Int. J. Coal Geol.* **2016**, *165*, 1–27. [CrossRef]

18. Moreno, T.; Trechera, P.; Querol, X.; Lah, R.; Johnson, D.; Wrana, A.; Williamson, B. Trace element fractionation between PM10 and PM2.5 in coal mine dust: Implications for occupational respiratory health. *Int. J. Coal Geol.* **2019**, *203*, 52–59. [CrossRef]
19. Kollipara, V.K.; Chugh, Y.P.; Mondal, K. Physical, mineralogical and wetting characteristics of dusts from Interior Basin coal mines. *Int. J. Coal Geol.* **2014**, *127*, 75–87. [CrossRef]
20. Trechera, P.; Moreno, T.; Córdoba, P.; Moreno, N.; Zhuang, X.; Li, B.; Li, J.; Shangguan, Y.; Kandler, K.; Dominguez, A.O.; et al. Mineralogy, geochemistry and toxicity of size-segregated respirable deposited dust in underground coal mines. *J. Hazard. Mater.* **2020**, *399*, 122935. [CrossRef] [PubMed]
21. Shangguan, Y.; Zhuang, X.; Querol, X.; Li, B.; Moreno, N.; Trechera, P.; Sola, P.C.; Uzu, G.; Li, J. Characterization of deposited dust and its respirable fractions in underground coal mines: Implications for oxidative potential-driving species and source apportionment. *Int. J. Coal Geol.* **2022**, *258*, 104017. [CrossRef]
22. Mischler, S.E.; Cauda, E.G.; Di Giuseppe, M.; McWilliams, L.J.; St. Croix, C.; Sun, M.; Franks, J.; Ortiz, L.A. Differential activation of RAW 264.7 macrophages by size-segregated crystalline silica. *J. Occup. Med. Toxicol.* **2016**, *11*, 57. [CrossRef] [PubMed]
23. Standards Association of Australia. AS 2985-2009. In *Workplace Atmospheres-Method for Sampling and Gravimetric Determination of Respirable Dust*; SAI Global: Brisbane, QLD, Australia, 2009.
24. Fandrich, R.; Gu, Y.; Burrows, D.; Moeller, K. Modern SEM-based mineral liberation analysis. *Int. J. Miner. Process.* **2007**, *84*, 310–320. [CrossRef]
25. Elmes, M. *The Characterisation of Airborne Particulate Matter by Automated Mineralogy: The Potential of the Mineral Liberation Analyser for the Monitoring of Mine-Derived Emissions*; The University of Queensland: Brisbane, QLD, Australia, 2020.
26. Abraham, J.L.; Crawford, J.A.; Scalzetti, E.; Kramer, L. Analysis of Lung Particle Burden in a 28 Year Old Man with Rapidly Progressive Coal Worker's Pneumoconiosis (Accelerated Silicosis). *Am. J. Respir. Crit. Care Med.* **2020**, *193*, 1.
27. Huang, X.; Li, W.; Attfield, M.D.; Nadas, A.; Frenkel, K.; Finkelman, R.B. Mapping and prediction of coal workers' pneumoconiosis with bioavailable iron content in the bituminous coals. *Environ. Health Perspect.* **2005**, *113*, 964–968. [CrossRef] [PubMed]
28. Zhang, Q.; Dai, J.; Ali, A.; Chen, L.; Huang, X. Roles of Bioavailable Iron and Calcium in Coal Dust-induced Oxidative Stress: Possible Implications in Coal Workers' Lung Disease. *Free. Radic. Res.* **2009**, *36*, 285–294. [CrossRef] [PubMed]